Acta Cryst. (1990). A46, 459-463

Image Deconvolution of a Single High-Resolution Electron Micrograph*

BY LIU YI-WEI, XIANG SHI-BIN, FAN HAI-FU,† TANG DONG AND LI FANG-HUA‡

Institute of Physics, Chinese Academy of Sciences, Beijing, China

PAN QING

Centre of Structure Analysis, University of Science and Technology of China, Hefei, China

AND N. UYEDA AND Y. FUJIYOSHI

Institute of Chemical Research, Kyoto University, Kyoto, Japan

(*Received* 20 *July* 1989; *accepted* 2 *January* 1990)

Abstract

An X-ray crystallographic method has been introduced into the image processing of high-resolution electron microscopy. This enables the deconvolution of single electron micrographs of a crystalline sample. For this purpose the chemical composition of the sample should be known approximately, the image should be taken near the optimum defocus condition, but no preliminary knowledge of the crystal structure is needed. The method has been proved to be efficient with a high-resolution electron micrograph of chlorinated copper phthalocyanine taken on the Kyoto 500 kV electron microscope.

* Part of this paper was presented at the IUCr Summer School on Crystallography and Its Teaching, Tianjin, China (1988).

† To whom correspondence should be addressed.

‡ Also at CCAST (World Laboratory), PO Box 8730, Beijing, China.

0108-7673/90/060459-05$03.00

© 1990 International Union of Crystallography

Introduction

Different procedures have been proposed for the deconvolution of high-resolution electron micrographs. Most of them use a series of micrographs with different defocus. Uyeda & Ishizuka (1974, 1975) first proposed a method of image deconvolution based on a single high-resolution electron micrograph. Later, Li Fang-hua & Fan Hai-fu (1979) reported an alternative method, which makes use of the direct method in X-ray crystallography. This method has been tested by Han Fu-son, Fan Hai-fu & Li Fang-hua (1986). It turns out that the method is efficient except in cases where the electron micrograph is taken near the optimum defocus condition. Hence it is important to have some method to fill this gap. On the other hand, procedures for the deconvolution using a single electron micrograph have so far been tested only by simulation. Hence in order to evaluate the method in practice a test on experimental electron micrographs is essential. In this paper, a new method is described which is particularly suitable for image deconvolution near the optimum defocus condition. Test results for an experimental electron micrograph are also given.

Principle

For a crystalline sample, the aim of image deconvolution should be to find correctly a set of structure factors whose Fourier transform will in turn yield the potential distribution function, *i.e.* the true structure image. Under the weak-phase-object approximation, in which the dynamic diffraction effect is neglected, the image intensities are related approximately to a set of structure factors by

$$I(\mathbf{r}) = 1 + 2\sigma\varphi(\mathbf{r}) * \Phi^{-1}[C(H)], \qquad (1)$$

here $I(\mathbf{r})$ is the image intensity at position $\mathbf{r}$ in real space. $\varphi(\mathbf{r})$ is the projection of the potential distribution function. Φ^{-1} and $*$ denote the inverse Fourier transform and convolution, respectively. $C(H)$ is the contrast transfer function which depends on the imaging and photographic conditions and is a real function of the magnitude of the reciprocal vector $\mathbf{H}$. $\sigma = \pi/\lambda U$, λ is the electron wavelength and U the accelerating voltage. Fourier transformation of (1) gives

$$\mathbf{T}(\mathbf{H}) = \delta(H) + 2\sigma\mathbf{F}(\mathbf{H})C(H), \qquad (2)$$

where $\mathbf{T}(\mathbf{H})$ is the Fourier transform of $I(\mathbf{r})$. $\delta(H)$ is a delta function with its maximum at $H=0$. $\mathbf{F}(\mathbf{H})$ is the structure factor with the reciprocal vector equal to $\mathbf{H}$. Equation (2) can be rearranged as below provided $H \neq 0$ and $C(H) \neq 0$.

$$\mathbf{F}(\mathbf{H}) = \mathbf{T}(\mathbf{H})/2\sigma C(H). \qquad (3)$$

By making use of (3) one can derive both the magnitude and the phase of $\mathbf{F}(\mathbf{H})$ from the Fourier transform of image intensities, $\mathbf{T}(\mathbf{H})$.

The magnitude of F(H)

Consider the average of $|\mathbf{F}(\mathbf{H})|^2$ within a narrow ring on the reciprocal plane with a mean radius equal to H; we have from (3)

$$\langle|\mathbf{F}(\mathbf{H})|^2\rangle_H \simeq \langle|\mathbf{T}(\mathbf{H})|^2\rangle_H / 4\sigma^2 C^2(H). \qquad (4)$$

On the other hand, as is well known in X-ray crystallography (Wilson, 1949) we have

$$\langle|\mathbf{F}(\mathbf{H})|^2\rangle_H \simeq \sum_{j=1}^{N} f_j^2(H), \qquad (5)$$

where $f_j^2(H)$ is the atomic scattering factor of the jth atom for X-rays, and N is the number of atoms in the unit cell. By replacing $f_j^2(H)$ with the atomic scattering factor for electrons, (5) can be used in the case of electron diffraction. From combination of (4) and (5) it follows that

$$C^2(H) \simeq \langle|\mathbf{T}(\mathbf{H})|^2\rangle_H / 4\sigma^2 \sum_{j=1}^{N} f_j^2(H). \qquad (6)$$

Substitute (6) into (3). The magnitude of $\mathbf{F}(\mathbf{H})$ can be expressed as

$$|\mathbf{F}(\mathbf{H})| = |\mathbf{T}(\mathbf{H})| \left[\sum_{j=1}^{N} f_j^2(H) \Big/ \langle|\mathbf{T}(\mathbf{H})|^2\rangle_H\right]^{1/2}. \qquad (7)$$

All the terms on the right-hand side of (7) are either known in theory or derivable from experimental measurement.

The phase of F(H)

It is evident from (3) that the phase of $\mathbf{F}(\mathbf{H})$ is equal to that of $\mathbf{T}(\mathbf{H})$ or 180° apart from it, depending on whether the sign of $C(H)$ is positive or negative. With the weak-phase-object approximation, $C(H)$ can be written as

$$C(H) = \sin\chi_1(H)\exp[-\chi_2(H)], \qquad (8)$$

in which

$$\chi_1(H) = \pi\Delta f\lambda H^2 + \tfrac{1}{2}(\pi C_S\lambda^3H^4),$$
$$\chi_2(H) = \tfrac{1}{2}(\pi^2\lambda^2H^4D^2),$$

where Δf is the defocus value, C_S is the spherical aberration coefficient and D is the standard deviation of the Gaussian distribution of defocus due to the chromatic aberration (Fejes, 1977). Obviously $\exp[-\chi_2(H)]$ is always positive. Hence only the term $\sin\chi_1(H)$ can cause a sign change of $C(H)$. In addition, since C_S is nearly constant for a given electron-optical system, the only active factor affecting the sign of $C(H)$ is Δf. It is well known in electron microscopy that there exists a certain value of Δf, *i.e.* the optimum defocus value, for which the sign of $\sin\chi_1$ does not change within a wide range of H.

Under the weak-phase-object approximation, $\sin \chi_1$ and hence the contrast transfer function $C(H)$ will be mostly negative if Δf is close to the optimum defocus value. Therefore we can write, according to (3),

$$\mathbf{F(H)} \simeq -\mathbf{T(H)}/2\sigma|C(H)|, \quad (9)$$

or

$$\theta_{\mathbf{F(H)}} \simeq \theta_{\mathbf{T(H)}} + \pi, \quad (10)$$

where θ denotes the phase angle. Combining (9) and (6), we have finally

$$\mathbf{F(H)} \simeq -\mathbf{T(H)}\left[\sum_{j=1}^{N} f_j^2(H) \Big/ \langle|\mathbf{T(H)}|^2\rangle_H\right]^{1/2}. \quad (11)$$

This forms the basis of image deconvolution using a single electron micrograph under the weak-phase-object approximation and the optimum defocus condition. As is evident in (11), all we need for obtaining a set of structure factors **F(H)** are the image intensity distribution on a single electron micrograph and the chemical composition of the crystalline sample.

Test and results

The experimental electron micrograph of the crystalline sample of chlorinated copper phthalocyanine ($C_{32}N_8Cl_{16}Cu$, $a = 19{\cdot}62$, $b = 26{\cdot}04$, $c = 3{\cdot}76$ Å and $\beta = 116{\cdot}5°$) is shown in Fig. 1, which was taken on the Kyoto 500 kV electron microscope with $\lambda = 0{\cdot}0142$ Å, $C_S = 1{\cdot}06$ mm, $D = 100$ Å and $\Delta f \simeq 500$ Å. The micrograph was digitized using the Perkin–Elmer PDS microdensitometer data acquisition system with 50×50 μm aperture. The two-dimensional unit cell ($a' = a \sin \beta = 17{\cdot}56$, $b = 26{\cdot}04$ Å) was divided into 110×124 pixels. Ten unit cells were measured and then averaged to give the image intensity distribution on a unit cell. A half-tone graphical representation of the digitized averaged image is shown in Fig. 2(*a*). Fourier transformation of averaged image yielded a set (48 in total) of two-dimensional **T(H)** at 2 Å resolution. Values of $-\mathbf{T(H)}$ are listed in Table 1 as $F_t(1)$. The deconvolution was then done on **T(H)** as follows. The **T(H)**'s were arranged in descending order of $|H|$. Each $|\mathbf{T(H)}|^2$ was averaged with ten neighbours (five on each side) to give the value of $\langle|\mathbf{T(H)}|^2\rangle$ which in turn was substituted into (11) to calculate the corresponding **F(H)**. The set of deconvoluted structure factors so obtained is shown in

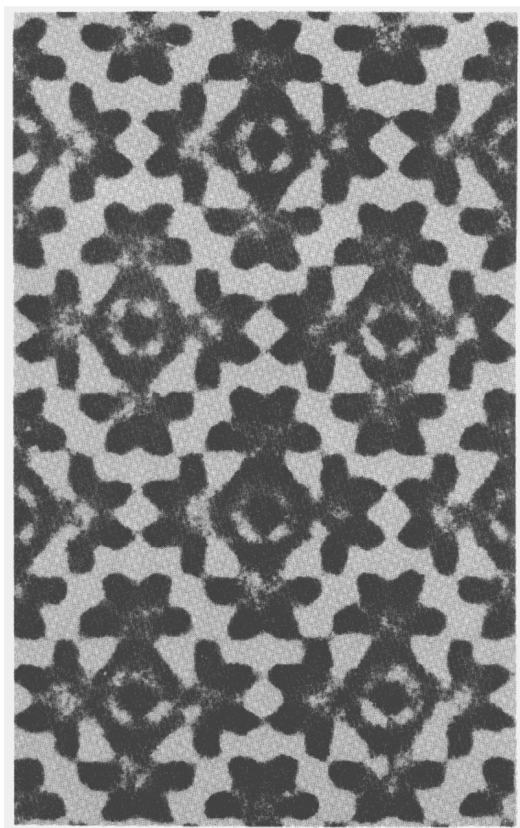

Fig. 1. The original micrograph of chlorinated copper phthalocyanine at 2 Å resolution.

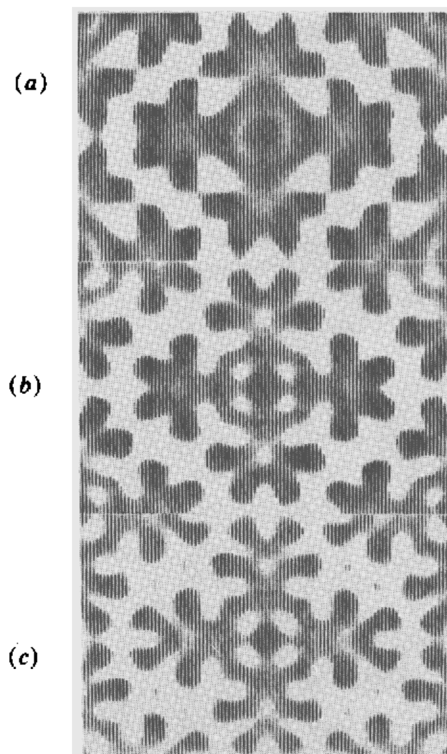

Fig. 2. Images of chlorinated copper phthalocyanine at 2 Å resolution. (*a*) Half-tone graphical representation of the digitized result of the original electron micrograph. (*b*) The deconvoluted image of (*a*). (*c*) The theoretical image.

Table 1. *Comparison of structure factors obtained from the 2Å electron microscopic image, the corresponding electron diffraction pattern and the structure model of chlorinated copper phthalocyanine*

h	k	$F_I(1)$	$F_I(2)$	F_D	F_M	h	k	$F_I(1)$	$F_I(2)$	F_D	F_M
2	0	0·649	0·673	0·637	1·116	5	5	1·124	0·857	0·925	1·401
4	0	−0·383	−0·319	0·577	−0·576	7	5	−0·024	−0·046	0·315	−0·061
6	0	−0·568	−0·448	0·889	−0·609	0	6	−0·559	−0·521	0·750	−0·375
8	0	−0·064	−0·128	0·228	−0·673	2	6	0·016	0·016	0·205	0·331
1	1	0·266	0·342	0·790	0·471	4	6	0·043	0·036	0·172	−0·412
3	1	1·117	1·294	0·810	0·493	6	6	0·289	0·422	0·299	−0·003
5	1	0·199	0·177	0·212	−0·136	1	7	0·844	0·671	0·633	0·456
7	1	0·583	0·604	0·873	1·795	3	7	1·358	1·071	0·984	1·151
0	2	0·366	0·419	0·832	1·162	5	7	−0·247	−0·282	0·592	0·478
2	2	−0·844	−0·949	1·087	−1·217	7	7	−0·200	−0·620	0·583	−1·472
4	2	0·163	0·147	0·152	0·522	0	8	−1·265	−0·986	1·027	−1·343
6	2	−0·064	−0·052	0·220	0·226	2	8	−0·419	−0·325	0·615	−0·358
8	2	0·197	0·398	0·533	0·449	4	8	0·940	0·914	0·998	1·243
1	3	−0·161	−0·171	0·830	−0·542	6	8	0·136	0·433	0·275	0·834
3	3	0·568	0·528	0·193	0·223	1	9	0·964	0·836	0·990	1·405
5	3	0·186	0·150	0·166	0·361	3	9	−0·145	−0·177	0·211	0·282
7	3	−0·235	−0·275	0·312	−0·554	5	9	−0·187	−0·791	0·702	−0·968
0	4	1·131	1·305	1·045	1·167	0	10	0·738	1·169	0·945	1·211
2	4	0·925	1·051	0·288	0·489	2	10	−0·001	−0·003	0·387	−0·435
4	4	−1·141	−1·006	0·863	−0·510	4	10	0·013	0·042	0·601	−0·845
6	4	0·490	0·426	0·721	0·393	1	11	0·182	0·378	0·647	0·597
8	4	−0·021	−0·065	0·169	0·625	3	11	0·054	0·170	0·261	0·363
1	5	0·137	0·128	0·363	0·217	0	12	−0·361	−1·142	0·965	−0·702
3	5	−1·751	−1·737	0·975	−1·123	2	12	0·049	0·150	1·039	0·820

$F_I(1)$: structure factors from the 2 Å electron microscopic image before deconvolution.
$F_I(2)$: structure factors from the 2 Å electron microscopic image after deconvolution.
F_D: structure-factor magnitudes from the diffraction pattern.
F_M: structure factors calculated from the structure model

Table 1 as $F_I(2)$. For comparison, a set of structure factors calculated from a model is given in Table 1 as F_M. The model is the same as that used by Kirkland, Siegel, Uyeda & Fujiyoshi (1985), which was estimated from the electron diffraction data (Uyeda, Kobayashi & Suito, 1972) and standard tables for bond lengths and angles for metal phthalocyanines. A set of structure-factor magnitudes measured from the electron diffraction pattern can be found in Table 1 as F_D. Among the four sets of 'structure factors' F_D and F_M are most similar to each other. However, the discrepancy between F_D and F_M, $R = \sum \| F_D| - |F_M\| / \sum |F_M|$, is still as large as 0·382. This is mainly due to the large experimental error on the diffraction measurement, the imperfection of the crystalline sample and the dynamic electron diffraction effect. The R factor for the structure factors before deconvolution, $F_I(1)$, with respect to F_M is 0·564 while that for the structure factors after deconvolution, $F_I(2)$, is 0·505. The R factor for $F_I(1)$ with respect to F_D is 0·468 while that of $F_I(2)$ is 0·394. Despite the unusually large values of R factor, the improvement gained from the deconvolution is obvious. This can be further confirmed in real space. The deconvoluted image was obtained by inverse Fourier transformation of $F_I(2)$. A half-tone graphical representation of the resulting image is shown in Fig. 2(b). The theoretical image calculated with F_M is shown in Fig. 2(c). As can be seen the theoretical image is much closer to the deconvoluted image than to the undeconvoluted one (Fig. 2a).

Discussion

The result can be made even better by improving the photographic recording technique. For example, the same image can be recorded on a series of photographs taken with different exposure times. This is an analogue of the multiple-film technique used in X-ray diffraction analysis.

While the present method is proposed for image deconvolution near the optimum defocus condition, it is not difficult to extend the method for use in cases far from this condition. By using (6) we can calculate an experimental curve of $C^2(H)$ from the image intensities and the chemical composition of the sample. On the other hand we can calculate a set of theoretical $C^2(H)$ curves which correspond to a series of Δf's with small interval. An appropriate Δf can be determined by finding out one of the theoretical curves, which is best fitted with the experimental curve. Substitute the corresponding calculated $C(H)$ into (3). A set of $\mathbf{F(H)}$ can then be calculated and the image deconvoluted.

In comparison with the previous method (Han Fu-son, Fan Hai-fu & Li Fang-hua, 1986) the present method is much simpler in calculation. When Δf is close to the optimum defocus value, this method can give much better results. However, when Δf is far from the optimum value, $\sin \chi_1$ will oscillate between +1 and −1 and will be sensitive to a small change of Δf. In this case the previous method will be superior to the present one. Hence it is recommended to use

both methods simultaneously whenever there is any doubt in practice.

References

FEJES, P. L. (1977). *Acta Cryst.* **A33**, 109–113.
HAN FU-SON, FAN HAI-FU & LI FANG-HUA (1986). *Acta Cryst.* **A42**, 353–356.
KIRKLAND, E. J., SIEGEL, B. M., UYEDA, N. & FUJIYOSHI, Y. (1985). *Ultramicroscopy*, **17**, 87–104.
LI FANG-HUA & FAN HAI-FU (1979). *Acta Phys. Sin.* **28**, 276–278.
UYEDA, N. & ISHIZUKA, K. (1974). Proc. 8th Int. Congr. Electron Microscopy, Vol. 1, pp. 322–323.
UYEDA, N. & ISHIZUKA, K. (1975). *J. Electron Microsc.* **24**, 65–72.
UYEDA, N., KOBAYASHI, T. & SUITO, J. (1972). *J. Appl. Phys.* **43**, 5181.
WILSON, A. J. C. (1949). *Acta Cryst.* **8**, 318–321.